Equilibrium properties of the reaction H2 ⇌ 2H by classical molecular dynamics simulations

ARTICLE *in* PHYSICAL CHEMISTRY CHEMICAL PHYSICS · DECEMBER 2013

Impact Factor: 4.49 · DOI: 10.1039/c3cp54149e · Source: PubMed

4 AUTHORS:

Ragnhild Skorpa
SINTEF
7 PUBLICATIONS **19** CITATIONS
SEE PROFILE

Jean-Marc Simon
University of Burgundy
83 PUBLICATIONS **675** CITATIONS
SEE PROFILE

Dick Bedeaux
Norwegian University of Science and Techn…
305 PUBLICATIONS **5,477** CITATIONS
SEE PROFILE

Signe Kjelstrup
Norwegian University of Science and Techn…
316 PUBLICATIONS **3,705** CITATIONS
SEE PROFILE

PCCP

PAPER

View Article Online
View Journal

Equilibrium properties of the reaction $H_2 \rightleftharpoons 2H$ by classical molecular dynamics simulations

Cite this: DOI: 10.1039/c3cp54149e

Ragnhild Skorpa,[a] Jean-Marc Simon,[b] Dick Bedeaux[a] and Signe Kjelstrup*[ac]

Received 1st October 2013,
Accepted 6th November 2013

DOI: 10.1039/c3cp54149e

www.rsc.org/pccp

We have developed a classical molecular dynamics model for the hydrogen dissociation reaction, containing two- and three-particle potentials derived by Kohen, Tully and Stillinger. Two fluid densities were investigated for a wide range of temperatures, and 11 fluid densities were considered for one temperature. We report the temperature range where the degree of reaction is significant, and also where a stable molecule dominates the population in the energy landscape. The three-particle potential, which is essential for the reaction model and seldom studied, together with the two-particle interaction lead to a large effective excluded volume diameter of the molecules in the molecular fluid. The three-particle interaction was also found to give a large positive contribution to the pressure of the reacting mixture at high density and/or low temperatures. From knowledge of the dissociation constant of the reaction and the fluid pressure, we estimated the standard enthalpy of the dissociation reaction to be 430 kJ mol^{-1} (ρ = 0.0695 g cm^{-3}) and 380 kJ mol^{-1} (ρ = 0.0191 g cm^{-3}). These values are in good agreement with the experimental vaule of 436 kJ mol^{-1} under ambient pressure. The model is consistent with a Lennard-Jones model of the molecular fluid, and may facilitate studies of the impact of chemical reactions on transport systems.

1 Introduction

By computer simulations one can study systems under conditions that are difficult to achieve in a laboratory. For instance, at very high temperatures, above 3000 K (at 1 bar), there is a significant dissociation of hydrogen into atoms,[1] but this is difficult to measure. Likewise, it is difficult to measure at 300 GPa where hydrogen becomes metallic.[2] Simulation techniques are indispensable in such cases. The aim of this paper is to find a simulation tool that can help address problems that arise when chemical reactions take place in the presence of gradients in pressure, temperature and concentration. This is the case in most chemical reactors.

To quantitatively model a chemical reaction requires quantum mechanics. Such models are computationally expensive, however, and allow no easy interaction with flow fields. The aim of this paper is therefore to help establish a classical model for a chemical reaction using equilibrium molecular dynamics. Doing this, we hope to facilitate future studies of reactions and transport in combination. A first effort in this direction was made by Xu *et al.*[3,24] in their study of the reaction $F_2 \rightleftharpoons 2F$. The interesting result was that transport properties, like thermal conductivity and diffusion coefficients of the components in the mixture, were largely affected by the presence of the chemical reaction. It is therefore of interest to examine to which degree this effect also applies to other systems.

We have chosen the hydrogen dissociation reaction as an example in the present work. The properties of hydrogen are for instance important for the envisioned hydrogen society.[4,5] A selective separation of hydrogen (H_2) from the main product stream of the water gas shift reaction is then central. Such a separation can occur *via* a palladium (Pd) membrane.[6–8] At the palladium surface, hydrogen dissociates into atomic hydrogen, and atoms are transported through the metal lattice.[6,7,9] At the other side, the reverse reaction takes place; molecular hydrogen is formed from atoms, and removed from the surface by an inert sweep gas. Equilibrium and transport data for simulations of these steps are not available, and are also not easily accessible from experiments. A classical model for the hydrogen dissociation reaction may facilitate the modelling of such coupled transport phenomena.

The purpose of this paper is therefore to establish a model for the chemical reaction ($H_2 \rightleftharpoons 2H$) using molecular dynamics simulations at equilibrium. The aim is to find the range of conditions where the reaction takes place, and where the molecular hydrogen fluid dominates.

Few equilibrium studies have been performed on the nature of chemical reactions using classical equilibrium molecular dynamics (EMD). Cummings and Stell[10] studied chemical reactions ($A + B \rightleftharpoons AB$) with the use of statistical mechanical models. To the

[a] Norwegian University of Science and Technology, Høgskoleringen 5, 7149 Trondheim, Norway. E-mail: signe.kjelstrup@ntnu.no; Tel: +47 7359 4179
[b] Laboratorie Interdisciplinaire Carnot de Bourgogne, UMR, CNRS-Université de Bourgogne, Dijon, France
[c] Process & Energy Laboratory, Delft University of Technology, Leeghwaterstraat 44, 2628CA Delft, The Netherlands

best of our knowledge, no thorough study of the equilibrium properties of the hydrogen dissociation reaction has been done. High temperature hydrogen dissociation has however been studied. In 1996 Magro *et al.* studied molecular dissociation in hot, dense hydrogen, using path-integral Monte Carlo.[11] Delaney *et al.* studied the liquid–liquid phase transition between the molecular and atomic fluid phases in high-pressure hydrogen using quantum Monte Carlo[12] in 2006. None of these studies contains three particle interactions, however. In 1978 Siegbahn and Liu[13] obtained a 3-dimensional potential energy surface for H_3. In 1992 and 1994 Diedrich and Anderson studied the barrier height,[14] and the potential energy surface,[15] respectively, of the reaction $H + H_2 \Leftrightarrow H_2 + H$ using quantum Monte Carlo calculations. Stillinger and Weber[16] studied equilibrium conditions for the dissociation of fluorine using a classical model of the reaction. They concluded that combinations of two- and three-particle potentials suffice to represent the main features of chemical binding. An other example of such three particle interactions is the Axilrod and Teller potential to describe dispersion interactions,[17] and the effect of this potential has been studied for binary fluids by Sadus.[18,19] A comparison of several many-body potentials for silicon (Si_n-clusters, n = 2–6) was studied by Balamane in 1992.[20] In 1998 Kohen *et al.*[21] gave analytic expressions for the two- and three-particle potentials of hydrogen in a study of reactions on silicon surfaces. We shall build on these works in an effort to obtain a good model for the reaction. Work has been done on the H_4 potential by Boothroyd *et al.*,[22] but given the results of Stillinger and Weber we restrict ourselves to the two- and three-particle interactions.

We shall examine the interaction energy landscape of the model derived from Kohen *et al.*,[21] characterizing its states and their occupancy in terms of pair correlation functions, at various temperatures, for a density just below the triple point and for a moderately compressed gas density. Focus will be given on the particular effects of three-particle interactions, which are seldom studied in molecular simulations. We shall see that they have interesting effects on the pair-correlation functions, and therefore on the properties of the reacting mixture. We shall discuss in detail the effect on the pressure. The pressure calculation from particle interactions in a mixture, where particles constantly are formed or disappear, is by no means trivial. In this context we shall benefit from the existing methodology.[3,23] The temperature variation of the reaction shall also be studied.

The paper has been organized as follows. First we present the details of the hydrogen potential in Section 2. Section 3 discusses the details of the molecular dynamics simulations. In Section 4 we give results for the pair correlation function, the system pressure, the dissociation constant and the reaction enthalpy. Conclusions are given in Section 5.

2 Interaction potentials

For the computer simulations, we need an analytical form of the potential which describes essential interactions between particles in the system, based on an acceptable approximation to the electronic ground state potential of the collection of atoms involved.[3,16,21,24] Following Stillinger and Weber,[16] we use an interaction potential, U, which is the sum of two- and three-particle interaction contributions:

$$U(\mathbf{r}_1, \ldots, \mathbf{r}_N) = \sum_{i<j} u_{(2)}(\mathrm{r}_{ij}) + \sum_{i<j<k} u_{(3)}(\mathbf{r}_i, \mathbf{r}_j, \mathbf{r}_k) \qquad (1)$$

where $u_{(2)}$ and $u_{(3)}$ are the two- and three-particle potentials, respectively, and $\mathbf{r}_i$ are the positions of the hydrogen atoms. The spherically symmetric pair potential, $r_{ij} = |\mathbf{r}_i - \mathbf{r}_j|$, describes the interaction between two particles, and defines the bonded and non-bonded pairs. The pair-potential used in the calculations was given by Kohen *et al.*:[21]

$$u_{(2)}(r) = \begin{cases} \alpha(\beta r^{-p} - 1)\exp\left[\dfrac{\gamma_2}{r - r_c}\right] & \text{if } r < r_c \\ 0 & \text{if } r > r_c \end{cases} \qquad (2)$$

where $\alpha = 5.59 \times 10^{-21}$ kJ, $\beta = 0.044067$ Å^p, $\gamma_2 = 3.902767$ Å, $r_c = 2.8$ Å and $p = 4$ are constants.[21] α is chosen such that the minimum of the potential gives the binding energy of hydrogen (432.065 kJ mol^{-1})[21] at the bond distance between two hydrogen atoms, $r_e = 0.74$ Å.[14] When the distance between two atoms is larger than the cut-off distance, $r \geq r_c$, the potential is zero. For convenience in the calculation procedures, reduced units based on the pair potential have been used. σ is defined by $u_{(2)}(\sigma) = 0$, which implies that $\sigma = \sqrt[6]{\beta} = 0.458$ Å. The value of ε, based on the bond energy of hydrogen, gives ε/k_B = 51 991 K. Thus, the reduced pair potential has a minimum of -1 at $r_{ij}^* = 1.6$.

The mass of one hydrogen atom, $m_0 = 1.67 \times 10^{-27}$ kg, is used to define the reduced total mass density $\rho^* = \rho\sigma^3/m_0$. This implies that the reduced total mass density equals the reduced total molar density in terms of $(N_H + 2N_{H_2})$. Reduced units are indicated by superscript *, and the relations between real and reduced units are given in Table 1.

The major role of the 3-particle potential is to prevent formation of more than one bond to each hydrogen atom. This is done by making it energetically non-favorable for a third atom to be close to two chemically bonded atoms. The three-particle potential given by Kohen *et al.*[21] is:

$$u_{(3)} = h_{i,j,k}(r_{ij}, r_{jk}, \theta_{i,j,k}) + h_{j,i,k}(r_{ji}, r_{ik}, \theta_{j,i,k}) + h_{i,k,j}(r_{ik}, r_{kj}, \theta_{i,k,j}) \qquad (3)$$

Table 1 Relations between reduced and real units, ε/k_B = 51 991 K, σ = 0.458 Å and $m_0 = 1.67 \times 10^{-27}$ kg

Reduced variable	Formula
Mass	$m^* = m/m_0$
Distance	$r^* = r/\sigma$
Energy	$u^* = u/\varepsilon$
Time	$t^* = (t/\sigma)\sqrt{\varepsilon/m_0}$
Temperature	$T^* = k_B T/\varepsilon$
Density	$\rho^* = \rho\sigma^3/m_0$
Pressure	$P^* = P\sigma^3/\varepsilon$
Velocity	$v^* = v\sqrt{m_0/\varepsilon}$

The h-functions are given by

$$h_{j,i,k}(r_{ji}, r_{ik}, \theta_{j,i,k}) = \begin{cases} \lambda a \exp\left[\dfrac{\gamma_3}{(r_{ji} - r_c)} + \dfrac{\gamma_3}{(r_{ik} - r_c)}\right] & \text{if } r_{ji} < r_c \text{ and } r_{ik} < r_c \\ 0 & \text{otherwise} \end{cases} \quad (4)$$

where

$$a = [1 + \mu \cos(\theta_{j,i,k}) + \nu \cos^2(\theta_{j,i,k})] \quad (5)$$

in real units, and $\lambda = 2.80 \times 10^{-21}$ kJ, $\mu = 0.132587$, $\nu = -0.2997$ and $\gamma_3 = 1.5$ Å are constants.[21] The cut-off distance, r_c, is the same for both the two- and three-particle interactions (2.8 Å).

In the triad subscript j, i, k the middle letter i refers to the atom at the subtended angle vertex. The distances have been written with respect to the center atom. The interaction energy is plotted for the triad j, i, k in Fig. 1 for a linear configuration of three hydrogen atoms. Only linear configurations of the three H atoms (j, i and k) are plotted, as it was established in the paper by Siegbahn and Liu that the linear configuration contained the lowest minima.[13] The figure shows three minima, taking the symmetry in the plot into consideration. The lowest minimum, $U_1^* = -0.999$, corresponds to the minimum seen for the pair potential, where two atoms (j and i) are chemically bonded, $r_{ji}^* = 1.6$, while the third atom (k) is far away, $r_{ik}^* = 6$. The second minimum, $U_2^* = -0.941$, shows that two atoms (j and i) are close, $r_{ji}^* = 2.2$, while the third atom (k) is located further away, $r_{ik}^* = 3.0$. The last minimum, $U_3^* = -0.906$, found on the symmetry axis, corresponds to distances $r_{ji}^* = r_{ik}^* = 1.9$. Such extra minima were not observed for fluorine.[16] We will comment on the second and the third minima in Section 4 (Results and discussion). The total potential was used to determine the distance of chemically bonded particles. When the distance between two particles was shorter than $r_{ji}^* \leq 4.0$ they were labeled as part of a molecule, see Fig. 1. This choice is in agreement with the procedure used by Stillinger and Weber,[16] and is further confirmed by the results for the pair correlation function in Section 4.

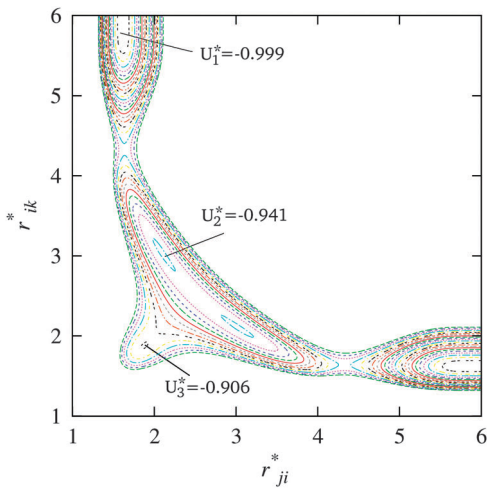

Fig. 1 Total interaction energy, U^*, for a linear configuration of 3 hydrogen atoms j, i and k as a function of the distances r_{ji}^* and r_{ik}^*. Three minima are observed, U_i^*, when the symmetry of the plot is taken into consideration. Reduced units are used, *cf.* Table 1.

3 Simulation details

The system consisted of 1000 hydrogen atoms (for all densities) in a non-cubic box with dimensions $L_x = 2L_y = 2L_z$, in the x, y and z direction, respectively. The volume of the box was $V = L_xL_yL_z = N_pm_0/\rho$, where ρ is the overall mass density ($\rho = N_pm_0/V$), N_p is the total number of particles ($N_p = N_H + 2N_{H_2} = 1000$) and m_0 is the mass of one hydrogen atom. Periodic boundary conditions were applied to the x-, y- and z-directions.[25] Data were sampled every 20 steps after the system had been equilibrated. A time step length of 0.1 in reduced units (0.22 fs), see Table 1, was used.

The velocity Verlet algorithm[26] was used to integrate Newton's equations of motion. A list of all pairs, which were closer to each other than a set distance, $r_{list}^* = 6.5$, was made to save computational time, as many particles are further away from each other than the cut-off distance, $r_c^* = 6.11$. Pair interactions were then only calculated when $r^* \leq r_{list}^*$. A similar algorithm, called NEIGHBOUR3, which was developed by Xu *et al.*,[3] was used to compute 3-particle interactions. In this algorithm a list of triplets is made by combining pairs from the pair list, which have one particle in common. As long as the displacement of the particles was less than half of $r_{list}^* - r_c^* = 0.4$, we did not need to update the two lists. This procedure avoided unnecessary calculation of particle interactions.

The program gave the temperatures in the box within ±0.1%. During the equilibration period the temperature was scaled to the set temperature every step by velocity scaling. After this, the temperature was adjusted every 100 steps, by scaling the velocities with the scaling factor given in eqn (6), to maintain the wanted temperature.[27]

$$\text{scale} = \sqrt{T_{inst}/T_{wanted}} \quad (6)$$

Here T_{inst} is the instantaneous temperature and T_{wanted} is the wanted temperature. This does not give a perfect canonical distribution, but we assume that the influence of this procedure on the calculated structural- and thermodynamic properties is negligible.

In order to test system size dependence, we repeated some of the equilibrium simulations for the same density with 4096 particles.

The pair correlation function along with the dissociation constant and reaction enthalpy was studied at a density just below the triple point density ($\rho^* = 0.004$) and approximately a fourth of this density ($\rho^* = 0.0011$), following the procedures of Stillinger and Weber.[16] For both densities temperatures were chosen in the range $0.003 \leq T^* \leq 0.3$. Additionally, a run was performed near the triple point of the molecular fluid ($\rho^* = 0.004$ and $T^* = 0.000268$).

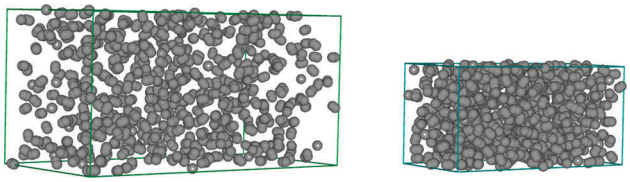

Fig. 2 Snapshot from simulations illustrating the density, $\rho^* = 0.0011$ (left) and $\rho^* = 0.004$ (right), at $T^* = 0.003$ ($T = 156$ K). A disordered system is clearly seen for both densities. Conditions are such that the dissociation is negligible.

For the calculation of the pressure (with the different contributions), densities in the range $0.00001 \leq \rho^* \leq 0.004$ were studied at $T^* = 0.03$. For the densities $\rho^* = 0.0011$ and 0.004 additional runs in a temperature range of $0.002 \leq T^* \leq 0.4$ were performed.

For the high density cases, $0.0003 \leq \rho^* \leq 0.004$, three million MD steps were used for equilibration of the system and the simulations were run a total of five million steps, including the equilibration. For the lower density cases, $0.00001 \leq \rho^* \leq 0.0001$, up to seven million MD steps were used for equilibration, and a total of up to ten million steps were used for the simulation run.

Fig. 2 shows snapshots from the simulations for the reduced densities $\rho^* = 0.0011$ (left) and $\rho^* = 0.004$ (right) at $T^* = 0.003$ ($T = 156$ K). We see that the high density system is a dense liquid, while the low density system can be compared to a compressed gas.

3.1 Calculation details

The temperature T was found from the average kinetic energy per degree of freedom of all particles:

$$T = \frac{1}{3k_B N_p}\sum_{i=1}^{N_p} m_i v_i^2 \tag{7}$$

where ${v_i}^2 = {v_{x,i}}^2 + {v_{y,i}}^2 + {v_{z,i}}^2$. From the virial theorem, the expression for the pressure in the presence of two- and three-particle interactions is:

$$P = \frac{k_B T N_p}{V} - \frac{1}{3V}\sum_{i=1}^{N_p}\left[\frac{1}{2}\sum_{j\ \text{pair with}\ i}\frac{\partial u_2(r_{ij})}{\partial r_{ij}} r_{ij} + \sum_{j<k\ \text{triplet with}\ i}\left(\frac{\partial h_{j,i,k}(r_{ji}, r_{ik}, \theta_{j,i,k})}{\partial r_{ji}} r_{ji} + \frac{\partial h_{j,i,k}(r_{ji}, r_{ik}, \theta_{j,i,k})}{\partial r_{ik}} r_{ik} + \frac{\partial h_{j,i,k}(r_{ji}, r_{ik}, \theta_{j,i,k})}{\partial r_{jk}} r_{jk}\right)\right] \tag{8}$$

The first term in eqn (8) is the ideal contribution to the pressure, while the second and the third terms give the contributions from the two- and three particle potentials, respectively. As the angle $\theta_{j,i,k}$, and the distance r_{ik} are constant in $h_{j,i,k}$ when we take the derivative with respect to r_{ji}, this derivative is easy to calculate; and similarly for the other two contributions. The contributions to the pressure will be calculated separately and compared.

In the calculation of the pressure we used the atomic method.[23] This implies that we took the kinetic contributions of all atoms to give the ideal contribution to the pressure, $N_p k_B T/V$. To this, we added force moments due to pair- and three-particle interactions from all atoms. Given that many atoms are part of a bound pair, one may ask whether the molecular method[23] is more convenient. Both methods are discussed in detail by Ciccotti and Ryckaert.[23] In the appendix of their article, they reproduce an unpublished proof given by Berendsen, showing that both definitions give the same pressure. As we calculate the forces, positions and velocities of all atoms in the MD simulation, it is natural to use the atomic method here.

The molar density, c_k, of component k is:

$$c_k = \frac{N_k}{N_A V} \tag{9}$$

where N_k is the number of particles of component k (H or H_2). Furthermore N_A is Avogadro's number. The mass density of the system can be found from

$$\rho = \frac{N_p m_0}{V} \tag{10}$$

The thermodynamic equilibrium constant, K_{th}, can be found from the dissociation constant, K_x, and the activity coefficients according to

$$K_{th} = \frac{x_H{}^2 \gamma_H{}^2}{x_{H_2}\gamma_{H_2}} \equiv K_x \frac{\gamma_H{}^2}{\gamma_{H_2}} \tag{11}$$

The equilibrium constant can then be used to find Gibbs energy of the reaction

$$\Delta_r G = \Delta_r G^\circ + RT \ln K_{th} \tag{12}$$

The standard reaction enthalpy can then be found from the van't Hoff equation at constant pressure

$$\left[\frac{\mathrm{d}\ln K_{th}}{\mathrm{d}(1/T)}\right]_P = -\frac{\Delta_r H^\circ}{R} \tag{13}$$

At chemical equilibrium, $\Delta_r G = 0$ and hence $\Delta_r G^\circ = -RT\ln K_{th}$. For an ideal mixture ${\gamma_H}^2/\gamma_H$ is unity and $K_x = K_{th}$. When the ratio of the activity coefficients at constant pressure is constant, we can find $\Delta_r H^\circ$ from the van't Hoff equation using K_x. We shall seek to find such conditions.

4 Results and discussion

4.1 Pair correlation functions

The atom–atom pair correlation function, $g(r)$, for the hydrogen atoms, including atoms that are part of a molecule, describes the correlation of two atoms as a function of the distance. A deviation in the pair correlation function from unity indicates correlations between particles due to intermolecular interactions. Hence, the pair correlation function gives information about the number of chemically bonded atoms and the distance between bonded atoms, and their neighboring atoms.[3,16]

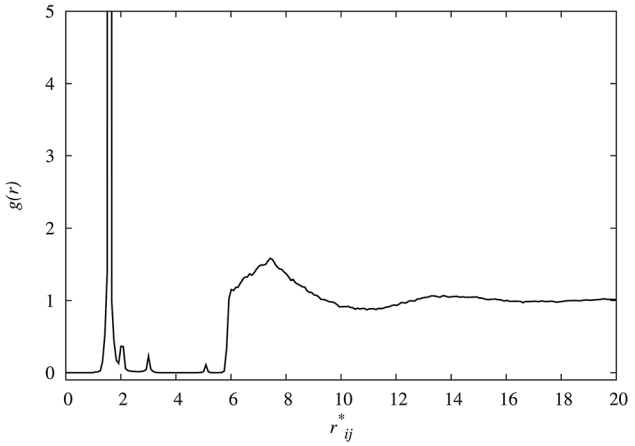

Fig. 3 Pair correlation function near the triple point of the molecular fluid. $T^* = 0.000268$ ($T = 14$ K), $\rho^* = 0.004$ ($\rho_H = 0.0695$ g cm^{-3}).

The pair correlation function near the triple point of the molecular fluid, $\rho^* = 0.004$ and $T^* = 0.000268$, is given in Fig. 3. The figure shows a very high peak at around $r_{ij}^* = 1.6$ and several minor peaks before a plateau is reached.

The high peak represents chemically bonded pairs and its area reflects the fact that there are 500 molecules in the system (no dissociation at this low temperature). The first three peaks in Fig. 3 can be directly related to Fig. 1, the potential energy of linear arrays of 3 hydrogen atoms. We see here that the distance $r_{ij}^* = 1.6$ corresponds to the arrangement with the lowest energy, $U_1^* = -0.999$. Two atoms are bound at this distance while the third atom is found at a distance $r_{ik}^* = 6$. This is compatible with the first high peak. This part is similar to the results of Stillinger and Weber for fluorine.[16] They observed no additional peaks in their pair correlation functions for fluorine, however, in agreement with one single minimum in their total potential.

The second minimum $U_2^* = -0.941$ in Fig. 1 leads to two small peaks in the pair correlation function in Fig. 3 at reduced distances $r_{ij}^* = 2.2$ and 3.0. The third minimum $U_3^* = -0.906$ in Fig. 1 has no clear impact on the pair correlation function in Fig. 3. The small peak at around $r_{ij}^* \approx 5$ cannot be traced to a minimum in the energy landscape. For a temperature of 14 K, the de Broglie wavelength for H is 10.15 in reduced units ($\Lambda = h/\sqrt{2\pi m_0 k_B T}$, where h is Planck's constant, and m_0 the mass of one hydrogen atom). For this temperature the classical calculation is therefore not adequate. The triplet structure is an artefact of this. In the simulations these linear formations of triplets, when they appear, are stable over the whole simulations, as the kinetic energy of the particles is too low to move to another minimum. We therefore interpret that the peaks below $r_{ij}^* = 4$ are due to intermolecular short-range order of chemically bonded pairs. The reason to do the classical calculation for this low temperature is to compare the results with the results for fluorine in the paper by Stillinger and Weber.[16] The similarity of the results validates our analysis.

It is interesting to observe that the system develops an effective excluded volume diameter. The pair potential is zero at a distance 1 in reduced units. When three-particle interactions are included, the molecule obtains an effective excluded volume diameter of about 6, as seen from Fig. 3, where the pair correlation function is approximately zero in the region $2.2 < r_{ij}^* < 6$, but rises sharply at 6. This value in real units is 2.748 Å, a value in good agreement with the value 2.7 Å given by Labet *et al.*[2] for the second shortest H–H separation at 1 GPa. Moreover, it compares well with the value 2.81 Å given by Allen and Tildesley[27] for a Lennard-Jones potential of molecular hydrogen. This means that our model for the chemical reaction at a meso-level is consistent with a coarser level fluid model of the molecular system, making this part of the model realistic.

Fig. 4 shows the pair correlation function at $T^* = 0.003$, for both $\rho^* = 0.004$ (Fig. 4(a)) and $\rho^* = 0.0011$ (Fig. 4(b)). When we compare the two pair correlation functions for the two densities in Fig. 4 we see that they have the same general trend. A large and narrow peak can be seen at $r_{ij}^* = 1.6$ in both cases. This

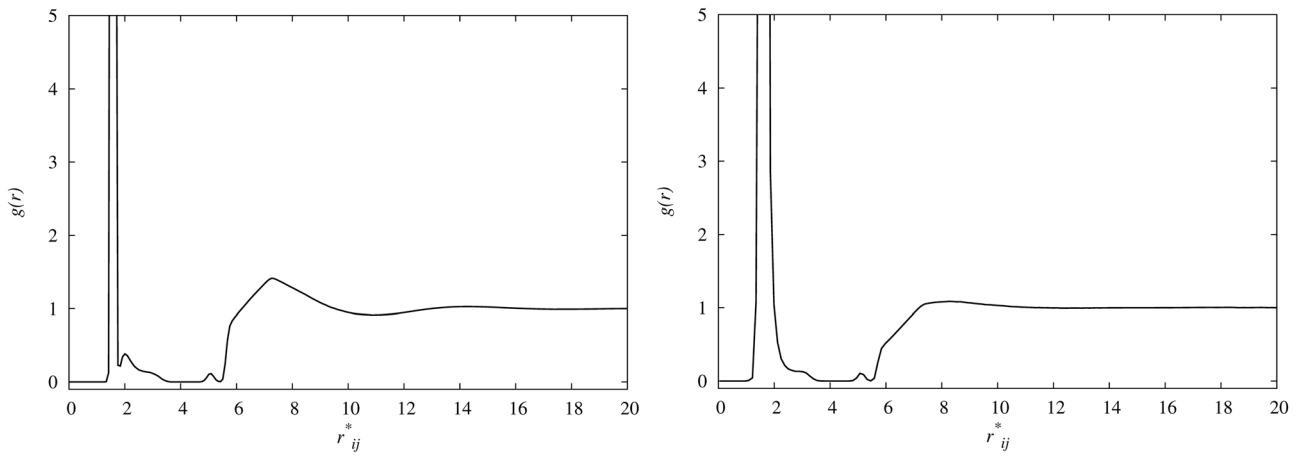

(a) $\rho^* = 0.004$ ($\rho = 0.0695$ g cm^{-3}) (b) $\rho^* = 0.0011$ ($\rho = 0.0191$ g cm^{-3})

Fig. 4 Pair correlation functions at $T^* = 0.003$ ($T = 156$ K). The high density, $\rho^* = 0.004$, is shown to the left (a) and the low density, $\rho^* = 0.0011$, to the right (b).

peak is broadest at the lower density ($\rho^* = 0.0011$, Fig. 4(b)). At the higher density ($\rho^* = 0.004$) it is just slightly broader than in Fig. 3. A broadening is also observed in the rest of the structure, when we compare Fig. 4(a) and (b) to the counterpart in Fig. 3. In the high density results, $\rho^* = 0.004$ in Fig. 4(a), the peak at $r_{ij}^* = 3$ has been incorporated into the small peak at $r_{ij}^* = 2.2$ as a shoulder. For the low density, $\rho^* = 0.0011$ in Fig. 4(b) a distinct extra peak is observed, but a broad shoulder remains. A broadening of peaks takes place, due to increase in the temperature as well as to the reduction in density. For a temperature of 156 K, the de Broglie wavelength for H is 3.03 in reduced units. For this temperature the classical calculation is therefore also not adequate. We refer to the discussion for 14 K above. The pair correlation function goes smoothly to unity as expected at about $r_{ij}^* = 10$ for the high density, and at about 8 for the low density. For neither density, dissociation was observed, *cf.* Tables 4 and 5.

The pair correlation function at $T^* = 0.03$ is given in Fig. 5, for the high density, $\rho^* = 0.004$ in Fig. 5(a), and for the low density, $\rho^* = 0.0011$, in Fig. 5(b). No dissociation was observed for either density, see Tables 4 and 5. The main peak at $r_{ij}^* = 1.6$, corresponding to the chemically bonded atoms, has further broadened for both densities compared to Fig. 4a and b. The two peaks due to the second potential minimum have disappeared. This is clearly due to the increase in the temperature. The area under the pair correlation function from $2.4 \leq r_{ij}^* \leq 5$ is zero for both densities. From r_{ij}^* around 9 the correlation function is roughly equal to one for both densities.

Fig. 6 shows the pair correlation functions for both the high density, $\rho^* = 0.004$ (Fig. 6(a)), and the low density, $\rho^* = 0.0011$ (Fig. 6(b)), at $T^* = 0.3$. The correlation function is near unity for $r_{ij}^* > 6$, as one should expect for this temperature. But the pair correlation is no longer zero when $2.2 < r_{ij}^* < 5$. This is a sign of the reaction taking place. If we compare the high- and low

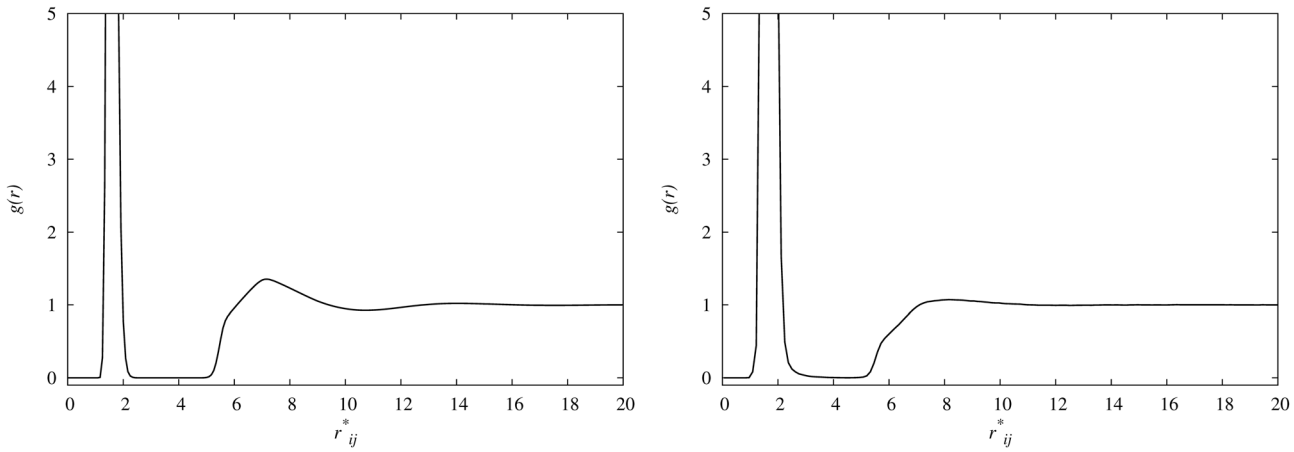

Fig. 5 Pair correlation functions at $T^* = 0.03$ ($T = 1560$ K). The high density, $\rho^* = 0.004$, is shown to the left (a) and the low density, $\rho^* = 0.0011$, to the right (b).

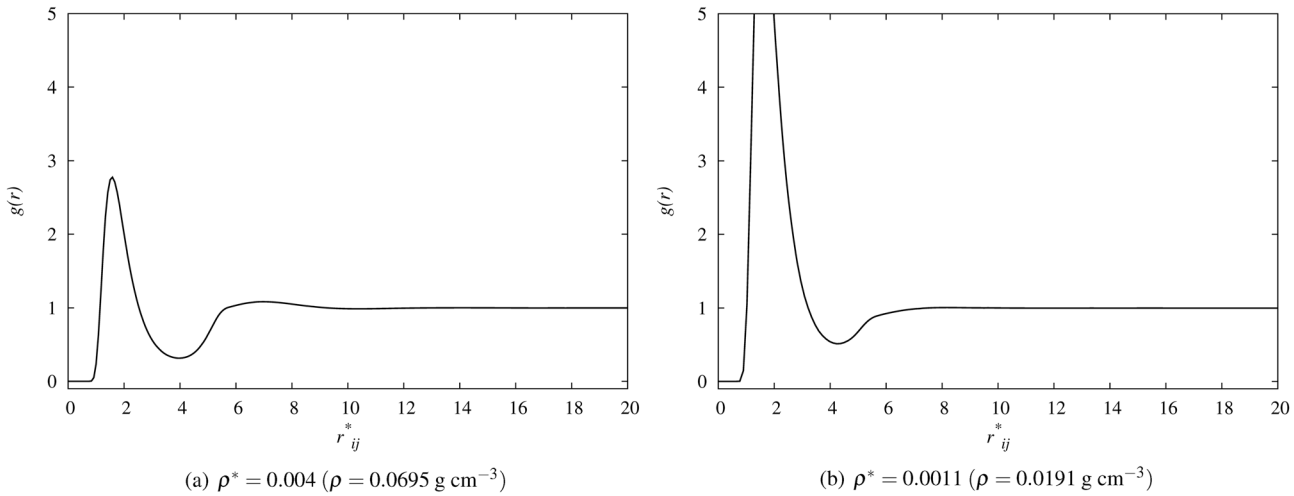

Fig. 6 Pair correlation functions at $T^* = 0.3$ ($T = 15\,600$ K). The high density, $\rho^* = 0.004$, is shown to the left (a) and the low density, $\rho^* = 0.0011$, to the right (b).

density figures, we see that the main difference is the intensity and broadness of the first peak, as the main peak in Fig. 6(b) is both broader and has a lower intensity than its high density counterpart. Compatible with this we find that more particles are bound at the low density. For the high density in Fig. 6(a), we observe 23% dissociation (232.4 atoms), while for the low density, in Fig. 6(b), a dissociation of 47% (468.7 atoms) is observed, *cf.* Tables 4 and 5.

In the counting procedure used, we label all particles as either atoms or molecules. If, during the simulation, the distance between two atoms is less than 4, they are labelled as molecules. At the end of every 20 time steps, we count the number of atoms. The rest is then counted as molecules. At higher temperatures, bonds are continuously formed and broken, and as Stillinger and Weber[28] say, this counting procedure will give a reasonable, but still approximate value of the number of molecules. We estimate the accuracy to be within ±1%.

In summary, from Fig. 3–6, we conclude that the three-particle potential has a large ordering effect on the molecules, in agreement with earlier observations.[16] The effective excluded volume diameter of the molecule becomes 6 in reduced units as a result of the three particle interaction, a value in agreement with the interparticle distance of the Lennard-Jones potential for molecular hydrogen.[27] The ordering effect was observed to decrease with increasing temperature.

At very low temperature (14 K and 156 K) quantum effects become important and for this reason our classical description leads to triplets which is an artefact of this. At very high temperatures, above 20 000 K, we see from the phase diagrams that we might be entering the plasma region of hydrogen.[29–31] At the highest temperature and density considered here (15 600 K and ρ = 0.0695 g cm^{-3}), we are however well within the region of the atomic fluid, and thus we expect that our model is able to predict the properties of hydrogen.

Under all conditions, bound particles were to be determined for a set distance $r_{ij}^* \leq 4$. For temperatures showing the behaviour illustrated by Fig. 6 we are dealing with a chemical reaction, and can find the fraction of molecules by counting the particles which obey this inequality. The role of the two- and three particle interactions will be examined further below.

4.2 The contributions to the pressure in a reacting mixture

The overall pressure, P_{tot}, in the calculation is a sum of the kinetic (or ideal) pressure, P_{ideal}, and the contributions from the two- and three particle potentials, P_{2part} and P_{3part}, see eqn (8). The relative magnitude of these contributions to the overall pressure at $T^* = 0.03$ was calculated and is given in Fig. 7 for densities in the range $0.00001 \leq \rho^* \leq 0.004$. The different contributions, P_i, to the pressure have been divided by the ideal pressure (P_i/P_{ideal}) to be able to compare the contributions at different densities relative to each other. As a consequence the ideal contribution, P_{ideal} (from the first part of eqn (8)) in Fig. 7 is equal to 1 for all densities. Important in Berendsen's proof of the equality of the atomic and molecular method for pressure calculations (see Ciccotti and Ryckaert[23]) is that the intramolecular two particle forces give a negative

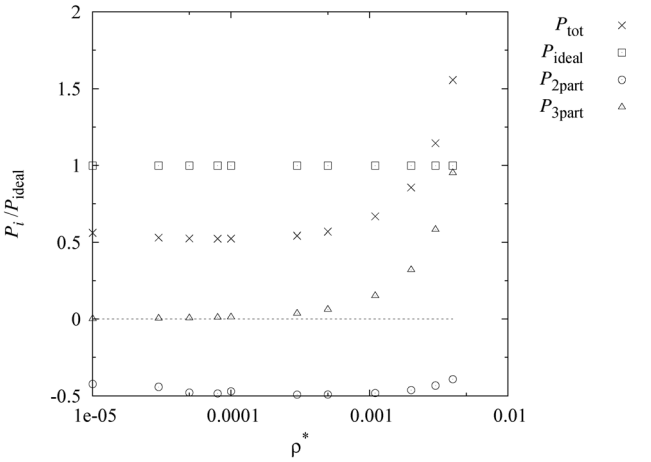

Fig. 7 The total pressure, P_{tot}, and the contribution from the ideal part, P_{ideal}, and two- and three particle interactions, P_{2part} and P_{3part} at $T^* = 0.03$ as a function of the density of the system, $0.00001 \leq \rho^* \leq 0.004$. The densities are plotted using a log scale. All pressures have been normalized with respect to the ideal pressure, giving $P_{ideal} = 1$ for all densities.

contribution to the pressure. In good approximation, it replaces the kinetic pressure of two atoms $2k_BT/V$ by the kinetic pressure of one molecule k_BT/V. It follows that the contribution to the pressure due to pair interaction is negative, and in essence reduces the kinetic pressure from $(N_H + 2N_{H_2})k_BT/V$ to $(N_H + N_{H_2})k_BT/V$. The contribution from the pair potential to the pressure in Fig. 7 is negative and approximately half the size of the ideal contribution, *cf.* ref. 23. So it is playing an important role in lowering the overall pressure.

The role of the three-particle interaction is very different. As we have seen from the pair correlation functions (see Section 4.1), no particles aside from the bound particles approach each other closer than almost a diameter of 6 in reduced units. This means that the effective excluded volume is almost $6^3 = 216$ times larger than that one would expect on the basis of the pair potential alone. This results in a large positive contribution to the pressure for a reduced density of the order of $1/216 \approx 0.005$ and above. For lower densities the contribution from the three particle interaction to the total pressure becomes less important, as can be seen in Fig. 7. In Fig. 7 we see that for densities less than $\rho^* = 0.0001$ the 3-particle interaction does not contribute significantly to the pressure. For the higher densities, the pressure increases with the density due to an increased contribution from the three-particle interactions. As for the pair potential contribution, it deviates significantly above $\rho^* = 0.005$ where molecules are on average in close contact. The three-particle interaction can therefore contribute significantly to the non-ideality of the mixture, even if a reaction does not take place to any significant degree as is the case in this plot. The contribution from the three-particle interaction under these conditions for our systems reflects that the higher the density becomes, the higher is the resulting repulsion without bond disruptions.

The influence of the temperature on the pressure at the densities $\rho^* = 0.004$ and $\rho^* = 0.0011$ was also investigated.

Table 2 The total pressure, P_{tot}, and the contributions to the pressure from the two- and three-particle interactions, P_{2part} and P_{3part}, as a function of temperature for $\rho^* = 0.004$. All data are normalized with respect to the ideal pressure, P_{ideal}, is 1 per definition for all cases, and is left out of the table. The accuracy was estimated to be 10% for $T^* < 0.03$ and a few percent for $T^* \geq 0.03$

T^*	0.000268	0.002	0.003	0.004	0.03	0.05	0.07	0.09
P_{tot}	1.92	1.77	1.73	1.72	1.55	1.50	1.46	1.43
P_{2part}	−5.7	−9.8	−5.6	−4.2	−0.39	−0.40	−0.41	−0.43
P_{3part}	6.6	10.5	6.3	4.9	0.95	0.90	0.88	0.87

T^*	0.15	0.17	0.2	0.23	0.25	0.3	0.4
P_{tot}	1.41	1.41	1.41	1.41	1.40	1.39	1.37
P_{2part}	−0.49	−0.51	−0.52	−0.52	−0.51	−0.48	−0.41
P_{3part}	0.91	0.92	0.93	0.92	0.91	0.87	0.78

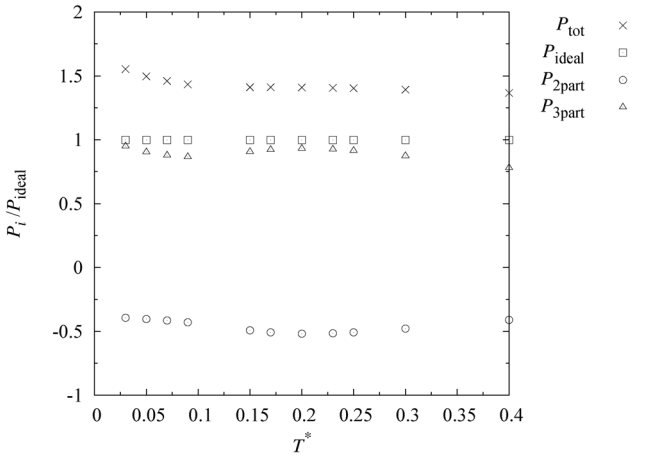

Fig. 8 The total pressure, P_{tot}, and the different contributions to the pressure, P_{ideal} and from the two- and three-particle interactions, P_{2part} and P_{3part} as a function of temperatures for the high density case, $\rho^* = 0.004$. All data have been normalized with respect to the ideal pressure, giving $P_{ideal} = 1$.

The range of temperatures covers the range where we can expect a significant degree of reaction, *cf.* next subsection. The results for the high density case, $\rho^* = 0.004$, where we can expect an impact of the reaction from $T^* = 0.07$ and upwards, are given in Table 2. For $T^* \geq 0.03$ the results are plotted in Fig. 8. All pressures have been normalized with respect to the ideal pressure (P_i/P_{ideal}), as before. This gives a normalized ideal pressure of 1 for all temperatures, which for this reason is left out of the table. The statistical error of the various pressures is in the order of a few percent, for $T^* < 0.03$ we estimate the statistical error of the two- and three-particle pressures (but not their sum) to be in the order of 10%.

In Table 2 we see that the normalized total pressure increases about 11% when the temperature is reduced by an order of magnitude. The sum of the normalized P_{2part} and P_{3part}, which equals the normalized total pressure minus 1, similarly increases when the temperature decreases. For T^* between 0.03 and 0.4 the change of the values of the normalized P_{2part} and P_{3part} is similarly rather small. The absolute value of these contributions is between zero and one for these temperatures. For lower temperatures the normalized P_{2part} and P_{3part} both increase by up to an order of magnitude without a similar increase in their sum. For these low temperatures, all hydrogen atoms are bound in molecules.

At low temperatures a particular property of this system affects the results. At these temperatures, there are no atoms in the system, and no reaction is going on. Most of the atoms, once they are bound to each other in a molecule, remain bound during the whole simulation. Concurrent with this is that also 3 atoms can arrive in the second minimum, see Fig. 1. The occurrence of such triplets was observed in Fig. 3 and 4 as small side peaks (shoulders) at reduced distances 2.2 and 3. The number of triplets is small, but they can remain stuck to each other during the whole simulation at low temperatures. The existence of some permanent triplets can explain the enormous decrease of the 2 particle contribution and roughly the same increase of the 3 particle contributions, while their sum is only slightly increased above the higher temperature value. The existence of triplets is a consequence of the potential we have used. The potential was an analytical representation of an energy surface generated from quantum mechanics,[16] but it may not represent reality under these extreme conditions. In Fig. 8, we only plot the normalized pressures for the high temperature domain, T^* between 0.03 and 0.4. The statistical error was estimated to be in the order of a few percent for $T^* \geq 0.03$. For lower temperatures the statistical error of the two- and three-particle pressures (but not their sum) was estimated to be in the order of 10%.

For the low density case, $\rho^* = 0.0011$, the total pressure and the different contributions to the pressure as a function of temperature are given in Table 3 below, and plotted in Fig. 9 for $T^* \geq 0.03$. Also here we can expect an impact of the reaction from $T^* = 0.07$ and up. From Table 3 we see that the normalized total pressure is essentially constant at low temperatures (between $T^* = 0.002$ and $T^* = 0.13$) and increases by about 20% when the reduced temperature increases to $T^* = 0.4$. This behavior is different from the result for the higher density, where the normalized total pressure decreased when the temperature increased. The sum of the normalized P_{2part} and P_{3part}, which equals the normalized total pressure minus 1, behaves

Table 3 The total pressure, P_{tot}, and the contributions to the pressure from the two- and three-particle interactions, P_{2part} and P_{3part}, as a function of temperature for $\rho^* = 0.0011$. All data are normalized with respect to the ideal pressure, P_{ideal}. The normalized ideal pressure, P_{ideal}, is 1 per definition for all cases, and is left out of the table. The accuracy was estimated to be 10% for $T^* < 0.03$ and a few percent for $T^* \geq 0.03$

T^*	0.002	0.003	0.004	0.03	0.05	0.07	0.09	
P_{tot}	0.69	0.69	0.68	0.67	0.66	0.66	0.67	
P_{2part}	−2.6	−1.9	−2.9	−0.48	−0.48	−0.48	−0.48	
P_{3part}	2.3	1.6	2.6	0.15	0.15	0.15	0.15	
T^*	0.11	0.13	0.15	0.17	0.2	0.25	0.3	0.4
P_{tot}	0.68	0.70	0.73	0.76	0.80	0.85	0.88	0.92
P_{2part}	−0.47	−0.44	−0.44	−0.42	−0.38	−0.32	−0.27	−0.20
P_{3part}	0.16	0.17	0.17	0.18	0.18	0.17	0.15	0.12

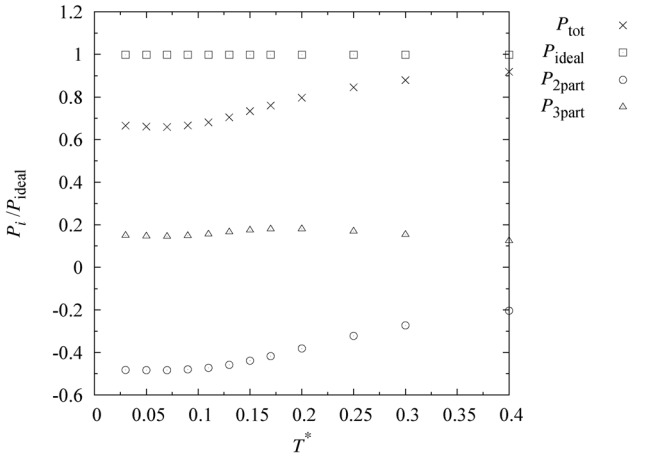

Fig. 9 The total pressure, P_{tot}, and the different contributions to the pressure, P_{ideal} and from the two- and three-particle interactions, P_{2part} and P_{3part} as a function of temperatures for the low density case, $\rho^* = 0.0011$. All data have been normalized with respect to the ideal pressure, giving $P_{ideal} = 1$.

similarly. The value of the normalized P_{2part} is reduced about 60% from $T^* = 0.03$ to $T^* = 0.4$, while the value of the normalized P_{3part} remains essentially constant in this temperature domain. For lower temperatures the normalized P_{2part} and P_{3part} both increase by up to an order of magnitude without a similar increase in their sum. The reason for this is the same as the one given for the higher density. In Fig. 9, we only plot the normalized pressures for the high temperature domain, T^* between 0.03 and 0.4.

For the high density, we see that the relative contributions to the normalized pressure are constant, up or down 10%, for $T^* = 0.03$–0.4, indicating that $\gamma_H{}^2/\gamma_{H_2}$ is approximately constant in this range. This indicates that we can use the van't Hoff equation, eqn (13), with K_x, to determine the standard enthalpy of the reaction, and we shall do so below. For the low density, we see the same trend in the normalized overall pressure for a lower temperature range, $0.03 \leq T^* \leq 0.13$, indicating that $\gamma_H{}^2/\gamma_{H_2}$ is also constant there.

For all temperatures, the effect of the three-particle potential is smaller in the low density case, compared to the ideal contribution and the contribution from two-particle interactions.

4.3 Dissociation constants and the enthalpy of reaction

The dissociation of hydrogen was studied as a function of temperature for two different densities, $\rho^* = 0.004$ and $\rho^* = 0.0011$, by counting the number of atoms every 20 steps. At the end, an average over the last 2000 steps was taken.

For the liquid like density, $\rho^* = 0.004$, the total pressure, the dissociation (number of H), mole fraction along with the calculated dissociation constants, K_x, are given in Table 4 below. From Table 4, we see that no dissociation is observed for $T^* \leq 0.05$ at $\rho^* = 0.004$. When we increase the temperature from $T^* = 0.05$ to $T^* = 0.4$, we see a large increase in the dissociation to 29%. As expected, since the main contribution

Table 4 Dissociation (N_H), mole fraction (x_i), total pressure (P^*) and the dissociation constant (K_x) for the high density, $\rho^* = 0.004$

T^*	0.000268	0.002	0.003	0.004	0.03	0.05	0.07	0.09
N_H	0.00	0.00	0.00	0.00	0.00	0.00	1.98	5.54
N_{H_2}	500.00	500.00	500.00	500.00	500.00	500.00	499.01	497.23
x_{H_2}	1.000	1.000	1.000	1.000	1.000	1.000	0.996	0.989
K_x	—	—	—	—	—	—	0.000	0.000
P^*	3×10^{-6}	1×10^{-5}	2×10^{-5}	3×10^{-5}	2×10^{-4}	3×10^{-4}	4×10^{-4}	5×10^{-4}
T^*	0.15	0.17	0.2	0.23	0.25	0.3	0.4	
N_H	66.90	91.42	137.61	172.42	192.39	232.42	288.50	
N_{H_2}	466.55	454.29	431.19	413.79	403.81	383.79	355.75	
x_{H_2}	0.875	0.832	0.758	0.706	0.677	0.623	0.552	
K_x	0.018	0.034	0.077	0.123	0.154	0.228	0.363	
P^*	8×10^{-4}	9×10^{-4}	1.1×10^{-3}	1.3×10^{-3}	1.4×10^{-3}	1.7×10^{-3}	2.2×10^{-3}	

Table 5 Dissociation (N_H), mole fraction (x_i), total pressure (P^*) and the dissociation constant (K_x) for the low density, $\rho^* = 0.0011$

T^*	0.002	0.003	0.004	0.03	0.05	0.07	0.09	
N_H	0.00	0.00	0.00	0.00	0.00	5.92	15.77	
N_{H_2}	500.00	500.00	500.00	500.00	500.00	497.04	492.11	
x_{H_2}	1.000	1.000	1.000	1.000	1.000	0.988	0.969	
K_x	—	—	—	—	—	0.000	0.001	
P^*	1×10^{-6}	2×10^{-6}	3×10^{-6}	2×10^{-5}	4×10^{-5}	5×10^{-5}	7×10^{-5}	
T^*	0.11	0.13	0.15	0.17	0.2	0.25	0.3	0.4
N_H	53.05	98.20	147.71	212.97	285.00	396.19	468.74	554.88
N_{H_2}	473.48	450.90	426.14	393.51	357.50	301.91	265.63	227.56
x_{H_2}	0.899	0.821	0.743	0.649	0.556	0.432	0.362	0.295
K_x	0.011	0.039	0.089	0.190	0.354	0.745	1.126	1.689
P^*	8×10^{-5}	1×10^{-4}	1×10^{-4}	1×10^{-4}	2×10^{-4}	2×10^{-4}	3×10^{-4}	4×10^{-4}

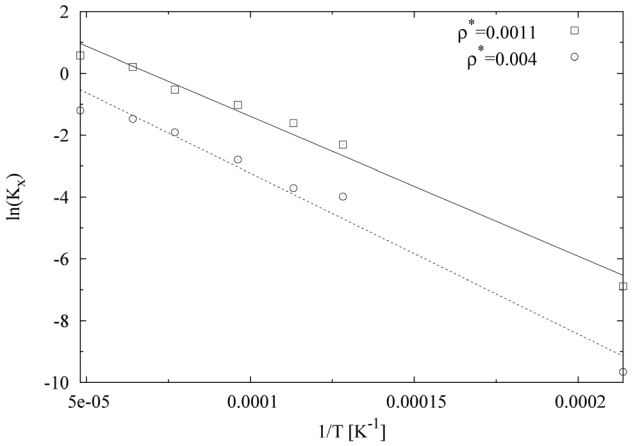

Fig. 10 The natural logarithm of the dissociation constant, $\ln K_x$, plotted as a function of the inverse temperature ($T^* = 0.09–0.3$).

to the pressure is the ideal pressure, the overall pressure increases with temperature.

The results for the dissociation, mole fraction, total pressure and the dissociation constant are given in Table 5 for the low density, $\rho^* = 0.0011$. From Table 5 we see that for $T^* \leq 0.05$ no dissociation is observed, while at $T^* = 0.09$ we observe almost 2% dissociation. Increasing the temperature further increases the dissociation up to 55% at $T^* = 0.4$. As expected the pressure increases with temperature. Comparing the dissociation for the high and low density a larger dissociation was observed for the low density for $T^* \geq 0.07$. As expected, the observed overall pressure is higher for the higher density.

Assuming that the ratio $\gamma_H{}^2/\gamma_{H_2}$ is constant, the logarithm of the dissociation constant, $\ln K_x$, as a function of $1/T$ was used to calculate the standard enthalpy of reaction, $\Delta_r H^\circ$, for temperatures where the reaction is significant, $0.09 \leq T^* \leq 0.4$. The results are plotted in Fig. 10 for both densities. An approximate linear trend is observed for both densities. For both densities a deviation can be observed from the linear trend. This deviation is caused by a pressure effect, as the pressure is not the same in all the simulations. This effect is however expected to be small and to not have a big effect on the calculation of the enthalpy. From the linear fit made to the Fig. 10, we have estimated the standard enthalpy of reaction to be $\Delta_r H^\circ = 430$ kJ mol^{-1} and $\Delta_r H^\circ = 380$ kJ mol^{-1} for the high- and low density, respectively. The standard enthalpy of reaction can be compared to the binding energy of H_2 (436 kJ mol^{-1} at 298 K and 1 bar).[1,21] At the moment, we are not able to determine the standard enthalpy of the reaction independently for each temperature, as we have no knowledge about the ratio of the activity constants.

5 Conclusion

We have seen in the preceding sections that a classical MD model is able to capture the essential properties of a chemical reaction at equilibrium; namely its dissociation, enthalpy of reaction, and pressure and temperature variations. This was made possible by adding to the pair potential a three-particle interaction potential. The system behaviour on the meso-scale, characterized here by pair correlation functions, was found to be compatible with a coarser scale description, where the pair potential is the sole potential needed. In particular, the effective excluded volume diameter of the molecule was in agreement with the Lennard-Jones diameter used by others[2,27] to model fluid hydrogen. For low temperatures (14 K and 156 K) the de Broglie wavelength was large compared to the binding distance. For these temperatures the classical calculation is not appropriate. The triplet state found in the calculation at these temperatures is an artefact of this.

For two densities, $\rho^* = 0.0011$ and $\rho^* = 0.004$, and a series of temperatures, the three-particle interaction was found to have a large positive impact on the overall pressure. Assuming that the activity coefficient ratio was constant, the standard enthalpy of the reaction was estimated from van't Hoff equation to be 430 kJ mol^{-1} ($\rho^* = 0.004$) and 380 kJ mol^{-1} ($\rho^* = 0.0011$).

We have thus seen that a reacting mixture can be well modelled in a classical way, if the temperature is not too low. This opens up the possibility for dealing with problems related to reaction, diffusion, heat conduction, even thermal diffusion, and interface transport, in problems which are central to chemical reactor (combustion) technology. This is in complete accordance with the view of Stillinger and coworkers.[16,21] To the best of our knowledge the idea of these authors has not been taken to the next steps yet. Neither has the impact of a three-particle interaction potential been discussed in the literature, see however ref. 3. A simple model for the chemical reaction as presented here for hydrogen will allow its introduction into fluid modelling at large. The model may facilitate simultaneous studies of reaction and diffusion under various non-equilibrium conditions, and serve as a benchmark for quantum mechanical calculations of reactions.

Acknowledgements

P. O. Åstrand is thanked for clarifying discussions concerning the potential and the resulting triplet structures. The authors are grateful to the Storforsk Project Transport no. 167336 from NFR and the Department of Chemistry, NTNU, for financial support.

References

1 A. F. Holleman, E. Wiberg and N. Wiberg, *Inorganic Chemistry*, Academic press, California, USA, 2001.
2 V. Labet, P. Gonzalez-Morelos, R. Hoffman and N. W. Ashcroft, A fresh look at dense hydrogen under pressure. I. An introduction to the problem, amd an index probing equalization of H-H distances, *J. Chem. Phys.*, 2012, **136**, 074501.
3 J. Xu, S. Kjelstrup and D. Bedeaux, Molecular dynamics simulations of a chemical reaction; conditions for local equilibrium in a temperature gradient, *Phys. Chem. Chem. Phys.*, 2006, **8**, 2017–2027.

4 C. E. Thomas, Fuel cell and battery electric vehicles compared, *Int. J. Hydrogen Energy*, 2009, **34**, 6005–6020.
5 F. T. Wagner, B. Lakshmanan and M. F. Mathias, Electrochemistry and the Future of the Automobile, *J. Phys. Chem. Lett*, 2010, **1**, 2204–2219.
6 T. L. Ward and T. Dao, Model of hydrogen permeation behavior in palladium membranes, *J. Membr. Sci.*, 1999, **153**, 211–231.
7 S. Yun and S. T. Oyama, Correlations in palladium membranes for hydrogen separation: a review, *J. Membr. Sci.*, 2011, **375**, 28–45.
8 R. Skorpa, M. Voldsund, M. Takla, S. K. Schnell, D. Bedeaux and S. Kjelstrup, Assessing the coupled heat and mass transport of hydrogen through palladium membrane, *J. Membr. Sci.*, 2012, **394–395**, 131–139.
9 T. P. Perng and J. K. Wu, A brief review note on mechanisms of hydrogen entry into metals, *Mater. Lett.*, 2003, **57**, 3437–3438.
10 P. T. Cummings and G. Stell, Statistical mechanical models of chemical reactions, *Mol. Phys.*, 1984, **51**, 253–287.
11 W. R. Magro, D. M. Ceperley, C. Pierleoni and B. Bernu, Molecular dissociation in hot, dense hydrogen, *Phys. Rev. Lett.*, 1996, **76**, 1240–1243.
12 K. T. Delaney, C. Pierleoni and D. M. Ceperley, Quantum monte carlo simulation of the high-pressure molecular-atomic crossover in fluid hydrogen, *Phys. Rev. Lett.*, 2006, **97**, 235702.
13 P. Siegbahn and B. Liu, An accurate three-dimensional potential energy surface for H_3, *J. Chem. Phys.*, 1978, **68**, 2457–2465.
14 D. L. Diedrich and J. B. Anderson, An accurate quantum monte carlo calculation of the barrier height for the reaction $H + H_2 = H_2 + H$, *Science*, 1992, **258**, 786–788.
15 D. L. Diedrich and J. B. Anderson, Exact quantum monte carlo calculations of the potential energy surface for the reaction $H + H_2 \rightarrow H_2 + H$, *J. Chem. Phys.*, 1994, **100**, 8089–8095.
16 F. H. Stillinger and T. A. Weber, Molecular dynamics simulation for chemically reactive substances. Fluorine, *J. Chem. Phys.*, 1988, **8**, 5123–5133.
17 B. M. Axilrod and E. Teller, Interaction of the van der Waals type between three atoms, *J. Chem. Phys.*, 1943, **11**, 299–300.
18 R. J. Sadus, Exact calculation of the effect of three-body Axilrod-Teller interactions on vapour-liquid phase coexistence, *Fluid Phase Equilib.*, 1998, **144**, 351–359.
19 R. J. Sadus, The effect of three-body interactions on the liquid–liquid phase coexistence of binary fluid mixtures, *Fluid Phase Equilib.*, 1998, **150**, 63–72.
20 H. Balamane, T. Halicioglu and W. A. Tiller, Comparative study of silicon empirical interatomic potentials, *Phys. Rev. B: Condens. Matter Mater. Phys.*, 1992, **46**, 2250–2279.
21 D. Kohen, J. C. Tully and F. H. Stillinger, Modeling the interaction of hydrogen with silicon surfaces, *Surf. Sci.*, 1998, **397**, 225–236.
22 A. I. Boothroyd, P. G. Martin, W. J. Keogh and M. J. Peterson, An accurate analytic H_4 potential energy surface, *J. Chem. Phys.*, 2002, **116**, 666–689.
23 G. Ciccotti and J. P. Ryckaert, Molecular dynamics simulation of rigid molecules, *Comput. Phys. Rep.*, 1986, **4**, 345–392.
24 J. Xu, S. Kjelstrup, D. Bedeaux and J.-M. Simon, Transport properties of $2F \rightleftharpoons F_2$ in a temperature gradient as studied by molecular dynamics simulations, *Phys. Chem. Chem. Phys.*, 2007, **9**, 969–981.
25 T. Ikeshoji and B. Hafskjold, Non-equilibrium molecular dynamics calculation of heat conduction in liquid and through liquid–gas interface, *Mol. Phys.*, 1994, **81**, 251–261.
26 W. C. Swope, H. C. Andersen, P. H. Berens and K. R. Wilson Wilson, A computer simulation method for the calculation of equilibrium constants for the formation of physical clusters of molecules: Application to small water clusters, *J. Chem. Phys.*, 1982, **76**(1), 637–649.
27 M. P. Allen and D. J. Tildesley, *Computer Simulation of Liquids*, Oxford University Press, New York, 1987.
28 F. H. Stillinger and T. A. Weber, Molecular dynamics study of chemical reactivity in liquid sulfur, *J. Phys. Chem.*, 1987, **91**, 4899–4907.
29 B. Militzer, W. Margo and D. Ceperley, Characterization of the state of hydrogen at high temperature and density, *Contrib. Plasma Phys.*, 1999, **39**, 151–154.
30 D. Saumon and G. Chabrier, Fluid hydrogen at high density: Pressure dissociation, *Phys. Rev. A*, 1991, **44**, 5122–5141.
31 B. Militzer and D. M. Ceperley, Path integral monte carlo simulation of the low-density hydrogen plasma, *Phys. Rev. E*, 2001, **63**, 066404.